Improving the Accuracy of Mangrove Species Discrimination using Object Based and High Spatial Resolution Imagery: A Case Study in Pak Phanang, Thailand

Watanakij, N.[1,2] and Vaiphasa, C.[1*]
[1]Department of Survey Engineering, Faculty of Engineering, Chulalongkorn University, Bangkok 10330 Thailand, E-mail: nagon@kku.ac.th
[2]Department of Computer Science, Faculty of Sciences, Khon Kaen University, Khon Kaen 40002, Thailand E-mail: chaichoke@hotmail.com
** Correspondence Author: Vaiphasa, C.*

Abstract
Detailed mangrove species maps are often required for proper management of mangrove forests. Recent reports on tropical mangrove species classification based on modern earth observation satellite data strongly support the potential use of remote sensing technology in mangrove forest management. Nevertheless, difficulty has remained in distinguishing between two dominant species, Rhizophora apiculata and Rizophora mucronata. The aim of this study is to improve the discrimination accuracy between these two species using an object-based classification method along with very high resolution, Quickbird images. Texture analyses and object-based classification were applied to the indistinguishable areas. The results showed an improvement in overall accuracy from 92% to 97%. Moreover, the producer's accuracy of Rhizophora apicularta and Rizophora mucronata increased from 68% to 94% and from 94% to 95%, respectively. This outcome supports the use of the proposed method for resolving confusion between the two species. Additional data such as physiological parameters and vegetation indices may also be integrated in future studies for more accurate results.

1. Introduction

Mangroves are mainly populated in the coastal areas in the tropical zone (Green, 1998) encompassing both marine and coastal ecosystems. Mangrove forests play an important role in both ecology (e.g., reducing the shoreline erosion rates and providing habitats for aquatic animals) (Heumann, 2011b) and supporting local economies (e.g., fisheries and tourism) (Green, 1998, Wang et al., 2004a, Huang et al., 2009). Knowledge of the composition and distribution of the mangrove varieties is important for sustainable management of these areas. Remote sensing is a method widely used for monitoring and mapping mangrove composition and distribution because of its cost-effectiveness (Green, 1998, Heumann, 2011b, Wang et al., 2004a, Wang and Sousa, 2009, Vaiphasa et al., 2006 and Koedsin and Vaiphasa, 2013). Moderate spatial resolution sensors such as SPOT (Green, 1998, Tong et al., 2004, Gao et al., 2004, Chauvaud et al., 2013, Thu and Populus, 2007, Almeida-Guerra, 2002 and Gao, 1999), Landsat (Green, 1998, Kovacs et al., 2001, Manson et al., 2001, Muttitanon and Triphati, 2005, Sirikulchayanon et al., 2008 and Alsaaideh et al., 2013) and Aster (Vaiphasa et al., 2006, Giri and Muhlhausen, 2008 and Saito et al., 2003) provide an effective tool for mapping the mangrove forests and tracking their changes (Kuenzer et al., 2011). So far, however, there has been little success in using these moderate resolution images to differentiate mangrove forests at the species level (Vaiphasa et al., 2006, Kuenzer et al., 2011, Koedsin and Vaiphasa, 2013, Myingt et al., 2008).

Very high resolution (VHR) satellite images that provide a clearer view of mangrove textures have been tested a number of times in past studies (Kuenzer et al., 2011). Specific image analyzing techniques such as neural network (Wang et al., 2008), texture analysis (Wang et al., 2004b), and fuzzy (Neukermans et al., 2008) were integrated in these studies so as to exploit the high resolution image information. Some methods have even incorporated VHR reflectance with Light Detection And Ranging (LiDAR) (Chadwick, 2011). Unfortunately, these studies were conducted on sub-tropical and high latitude zones that comprised only 2-3 mangrove species (i.e., *Black*, *Red* and *White*

mangroves) (Wang et al., 2004a, Wang et al., 2008, Wang et al, 2004b and Neukermans et al., 2008). Additional species varieties as found in the tropical zones would lead to more confusion in the spectral reflectance and result in lower classification accuracy (Vaiphasa et al., 2006 and Neukermans et al., 2008). There has been one recent study which attempted to deal with the complexity of five tropical mangrove species (Koedsin and Vaiphasa, 2013). The overall classification accuracy of the study reached 92% when using complex image processing techniques on hyperspectral satellite imagery (Koedsin and Vaiphasa, 2013). However, results regarding separability between two dominant species (*Rhizophora apiculata* and *Rizophora mucronata)* was inconclusive (Koedsin and Vaiphasa, 2013).

Fortunately, the two mangroves species in question have different leaf shapes (Tomlinson, 1995). It can therefore be hypothesised that leaf texture information may be extracted and utilized via a process of object-based classification (Li et al., 2010). Thus, the aim of this study is to incorporate leaf information into the classification process for improving mangrove classification accuracy, specifically, for the two species which are indistinguishable using current methods (*Rhizophora apiculata* and *Rizophora mucronata*). The study area is the Pak Phanang mangrove forest of Southern Thailand which is densely covered by five different tropical mangrove species (*Avicennia alba, Avicennia marina, Bruguiera parviflora, Rhizophora apiculata and Rhizophora mucronata*).

The Quickbird high-resolution image was chosen for this study. The final classification results were statistically tested against an independent testing data set using a data rotation method.

2. Materials and Methods

2.1 Study Area

The study area is the Pak Phanang District, Nakorn Sri Thammarat Province in southern Thailand as shown in Figure 1. Its mangrove forests comprise five dominant species including *Avicennia alba (Aa), Avicennia marina (Am), Bruguiera parviflora (Bp), Rhizophora apiculata (Ra)* and *Rhizophora mucronata (Rm)* (Koedsin and Vaiphasa, 2013). *Ra* is the most dominant species in the area as it covers around one third of the entire bay area followed by *Rm* (Vaiphasa et al., 2006 and Koedsin and Vaiphasa, 2013).

2.2 Data

2.2.1 Classified image

The most recent study cited earlier (Koedsin and Vaiphasa, 2013) utilized the potential of hyperspectral satellite imaging algorithms and the Spectral Angle Mapper (SAM) classifier to map mangrove tree species of the Pak Phanang area. In the current study, masked areas covered by the two species indistinguishable (*Ra* and *Rm*) using Hyperion image were created from the previously classified map derived by (Koedsin and Vaiphasa, 2013). These masked areas were used for object-based classification in the following sections. See the masked areas in Figure 2.

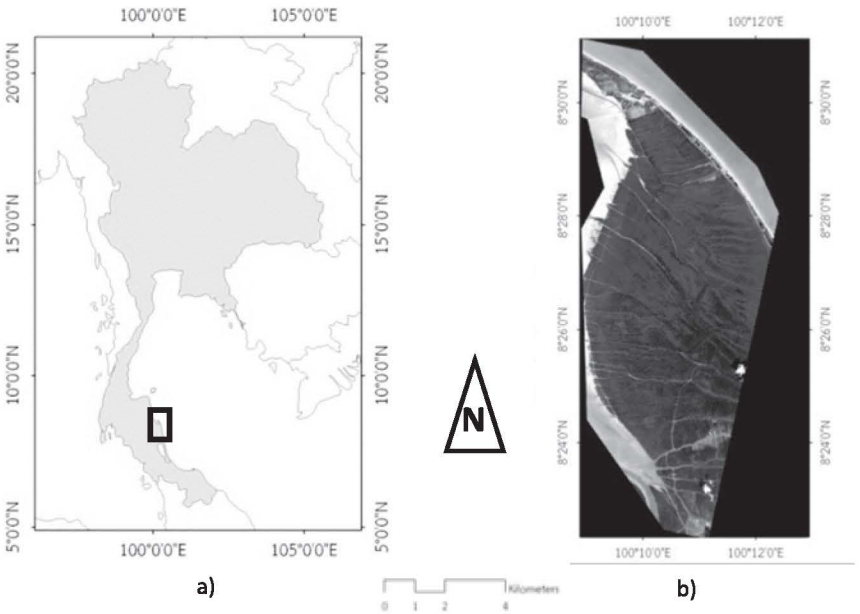

Figure 1a: Pak Phanang District, Nakorn Sri Thammarat Province, Thailand b) Quickbird image of the study area

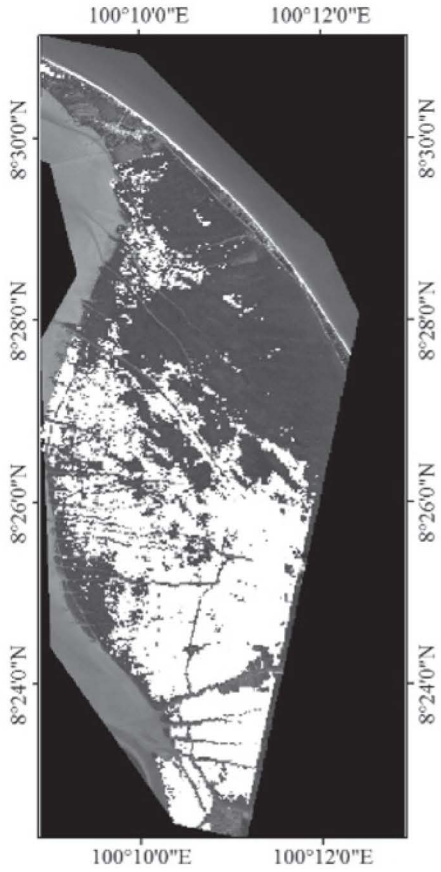

Figure 2: Mask areas displayed as a white polygon

2.2.2 Quickbird image

The Quickbird image was acquired on 13 October 2009 (See Figure 1). It consists of 4 multispectral bands with 2.4 meters spatial resolution. The image was radiometrically corrected and recorded at level 2A, in a 16-bit format. Then, the image was transformed to spectral radiance for atmospheric correction through MODTRAN4 incorporating FLAASH using ENVI 4.7 software. The data was orthorectified and resampled with a nearest neighbor method. The positional error of the resampling process was less than 1 pixel. Finally, the coverage of the two indistinguishable species, *Ra* and *Rm*, was masked at this stage using the previously classified image derived by (Koedsin and Vaiphasa, 2013).

2.2.3 Field data

The field data were collected from the study area between February and March 2011. A total 402 plots of mangrove trees were recorded for training and testing samples. Each field plot size was chosen at 30 x 30 meters according to the spatial resolution of the EO-1 Hyperion. The dominant tree species name and coordinates in the UTM system of each plot were recorded. Then, all plots were grouped into 5 classes by the dominant tree species in each plot as *Aa, Am, Bp, Ra* and *Rm*. The field samples were finally divided in half for the purpose of image classification and validation in the following stage (See Table 1).

Table 1: Amount of training and testing samples for each mangrove species

Mangrove Species	**Train**	**Test**
Avicennia alba (Aa)	44	44
Avicennia marina (Am)	30	30
Bruguiera parviflora (Bp)	38	38
Rhizophora apiculata (Ra)	51	51
Rhizophora mucronata (Rm)	38	38
Total	**201**	**201**

To prevent data bias, the training and testing samples were randomly divided 30 times (e.g., data rotation). The time difference between the acquisition of the image and the collection of the field data should be noted. This 16 month difference is deem to be of little significance to the successional process of the tropical mangroves (Hogarth, 1999 and Tomlinson, 1995).

2.3 Object-Based Classification

Given the selected areas of the indistinguishable species (See § 2.2.2), the following 3 steps of image classification (e.g., segmentation, object features and classification) were utilized.

2.3.1 Segmentation image

The Quickbird image was separated into segments by clustering adjacent pixels with similar reflectance and spatial characteristics (Heumann, 2011b and Almeida-Guerra, 2002). Thus, using commercial software (ENVI EX), the homogeneous area was represented by the large objects in the image, whereas the smaller objects represented the heterogeneous areas. The edge-based algorithm was chosen in this study which guaranteed that all objects were closed without losing any small patches. The trial and error scheme had to be applied because of the difficulty of defining the actual size of the mangrove canopies. The scale parameters were therefore adjusted starting from 50 to 100 per each training data set under a data rotation scheme.

2.3.2 Attributes

Three attributes including spatial, spectral, and texture were applied to the derived objects under

study. The spatial attribute included area, perimeter, and convexity. The spectral attribute included mean, minimum, maximum and standard deviation computed for each of the Quickbird bands (Saito et al., 2003). The four texture features were range, mean, variance and entropy. The texture filter of 13 x 13 pixels was used for moving window size (i.e., equal to the size of a field plot). All attributes were then combined in various ways to create six different combinations: 1) Spatial & Spectral & Texture; 2) Spatial; 3) Spectral; 4) Spatial & Texture; 5) Spatial & Spectral; and 6) Spectral & Texture.

2.3.3 Classification

The K-Nearest Neighbor (KNN) classifier (Hardin and Thomson, 1992) was applied through the segmented image which set parameter k to 1. The classification was done for 30 training sets for each scale and attribute factors to find the optimal results (i.e., data rotation). It should be noted that the proposed object-based techniques were only aimed at reducing the confusion between the two problematic classes (*Ra* and *Rm*). Then, at the final stage, the classified results were to be combined with the other three species for the purpose of validation (Koedsin and Vaiphasa, 2013).

2.4 Accuracy Assessment

The overall accuracy was calculated by comparing the classification results with the independent ground truth data of five mangrove classes. In addition, the quantity and allocation disagreement values were derived from the confusion matrix. Despite the redundancy and misleading concepts of the classical Kappa statistics (Pontius and Millones, 2011), a Kappa was calculated, because of its popularity, for measuring statistical agreement of classification results outside the diagonal line of the confusion matrix.

2.5 Statistical Analysis

2.5.1 One-way ANOVA analysis

Analysis of variance (ANOVA) is the technique used for determining the difference between means of multiple experiment groups (Gray and Kinnear, 2012). The null hypothesis states that there is no difference in any of the experiment's means (H_0:μ_1= μ_2 =μ_3=… μ_n). Therefore, rejecting the null hypothesis proves at least a couple of means to be different. If the null hypothesis is rejected, the Tukey's HSD (post-hoc) will be carried out to judge which groups of the experiment are the cause of rejection. In this study, the means of the overall classification accuracy were tested via ANOVA.

2.5.2 Z-test

Despite the criticism (Allouche et al., 2006 and Foody, 2004, 2008), the Z-test was conducted so as to compare between the kappa statistics extracted from the confusion matrices calculated in the previous classification section. The kappa values were compared, given the null hypothesis H_0 :(K_1 – K_2)=0 and the alternate hypothesis H_1 :(K_1 – K_2) ≠ 0, where H_0 is rejected if $Z \geq 1.96$ (i.e., at the 95% confidence level) (Congalton and Green, 2009). The Z statistic was calculated as shown in the following equation.

$$Z = \frac{|K_1 - K_2|}{\sqrt{Var(K_1) + Var(K_2)}}$$

Equation 1

3. Result

After computing with different segmentation scales, it was found that the scale factor 80 gained the highest overall classification accuracy. This scale level was therefore selected for the following operations. Six different attribute features at this scale factor were extracted and classified as displayed in Figure 3. The highest classification accuracy was reported when the spectral and texture features were combined together. It should be noted that a data rotation scheme was applied at this stage (i.e., repeating the calculation for 30 times with rotated samples). The influence of the data rotation can be noticed as error bars in Figure 3. The ANOVA test indicated that there were significant differences in at least one pair of six attribute features (p-value < 0.05). The superiority of the best combination (i.e., spectral and texture features) was also supported by the post-hoc test (p-value < 0.05) which revealed that the spectral and texture attribute feature combination was different from other combinations. For the purpose of visualization, the detailed classification results of the best feature combination are shown in Table 3.

Again, it should be noted that the classification preforming at this stage was designed to distinguish between the two indistinguishable classes, (*Ra* and *Rm*). Thus, Table 2 displays only the classification results between the two classes. The classification results of the two classes were to be re-combined with the other three classes (*Aa, Am* and *Bp*) in the next stage of the experiment. The other three species were then re-combined so as to produce confusion matrices. The best overall accuracy was found at 97%. This best confusion matrix (Table 3a) is shown in comparison with the earlier confusion matrix in Table 3b (i.e., the classification results produced by the use of the reflectance data of the Hyperion image alone (Koedsin and Vaiphasa, 2013).

Table 2: Classification records of the two indistinguishable classes when the best feature combination (spectral and texture features) was used in the data rotation process (i.e., 30 runs). The 26th iteration gained the highest classification accuracy of 95% (highlighted in grey).

Iteration	OA-Test (%)	Kappa	Iteratio	OA-Test (%)	Kappa
1	88%	0.76	16	90%	0.80
2	90 %	0.81	17	90%	0.80
3	87%	0.74	18	92%	0.84
4	92%	0.84	19	89%	0.78
5	91%	0.82	20	91%	0.82
6	87%	0.76	21	92%	0.83
7	88%	0.77	22	93%	0.85
8	86%	0.75	23	91%	0.82
9	87%	0.76	24	91%	0.82
10	91%	0.83	25	88%	0.76
11	88%	0.77	**26**	95%	0.90
12	89%	0.78	27	89%	0.78
13	88%	0.76	28	92%	0.83
14	88%	0.76	29	88%	0.76
15	88%	0.77	30	88%	0.77

Table 3a: Confusion matrix of the re-combined class information and (b) the confusion matrix of the original pixel-based classification

(a)	survey							(b)	survey						
	Rm	*Ra*	*Am*	*Aa*	*Bp*	PA	UA		*Rm*	*Ra*	*Am*	*Aa*	*Bp*	PA	UA
Rm	36	1	0	1	0	95%	95%	*Rm*	26	2	0	1	0	68%	90%
Ra	2	49	0	0	0	96%	96%	*Ra*	12	48	0	0	0	94%	80%
Am	0	0	44	0	1	100%	98%	*Am*	0	0	44	0	1	100%	98%
Aa	0	1	0	29	0	97%	97%	*Aa*	0	1	0	29	0	97%	97%
Bp	0	0	0	0	37	97%	100%	*Bp*	0	0	0	0	37	97%	100%
Overall accuracy = 97% kappa = 0.96*								Overall accuracy = 92% kappa = 0.89							
* statistic significant								PA=Producer's Accuracy, UA=User's Accuracy							

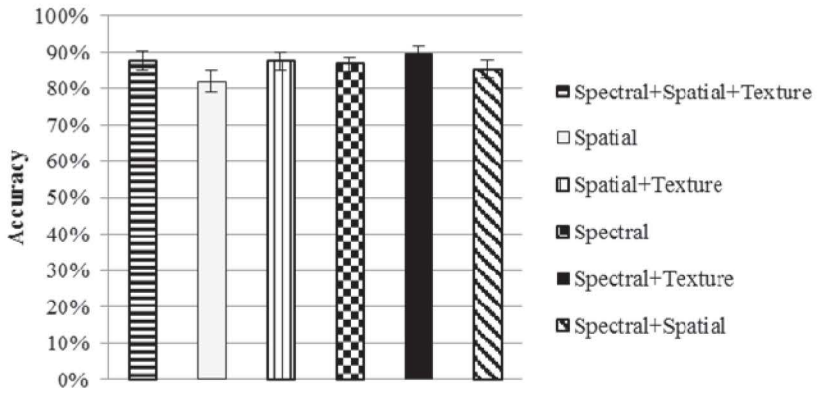

Figure 3: Bar charts of the average overall classification accuracy and standard deviation (small black error bars) of six different attribute features using the segmentation scale factor 80

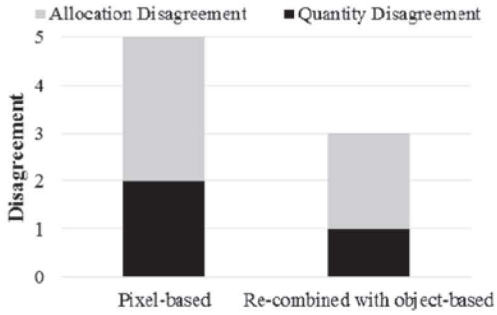

Figure 4: Bar chart of allocation and quantity disagreement of original pixel-based and re-combined with object-based classification

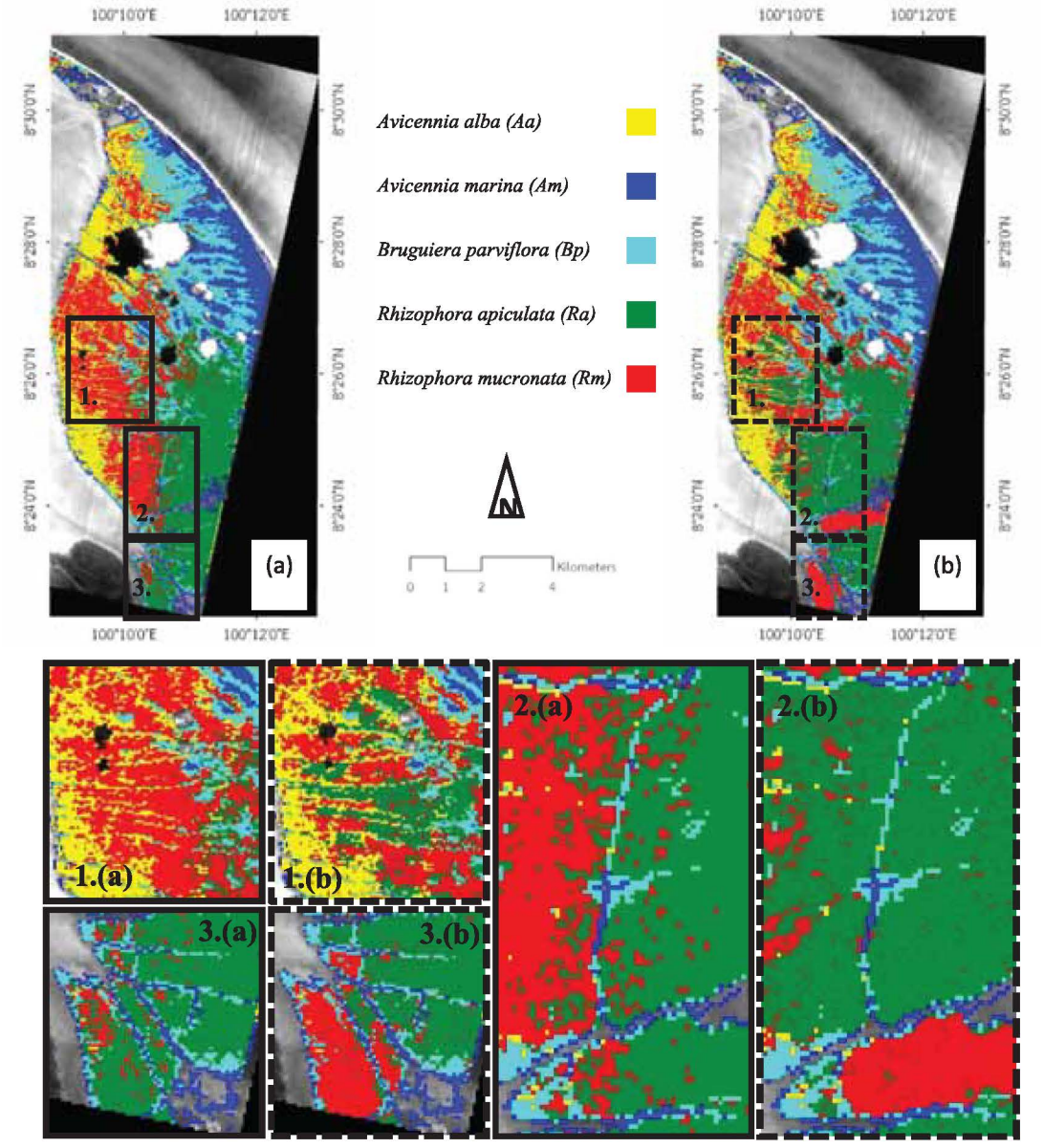

Figure 5: Classified map of original hyperspectral treatments (a) and the classified map of the proposed object-based method (b). The Magnified views show the two indistinguishable classes which were noticeably changed

The improvement can be marked in the producer accuracy of Ra and Rm. The producer accuracy of Rm improved from 68% to 94%. In addition, the producer accuracy of Ra improved from 94% to 95%. Next, the Z-test results of kappa statistics supported the improvement of the accuracy (p-value < 0.01). The classified maps of the re-combined object method and the original one are displayed in Figure 5a and 5b, respectively. Finally, the quantity and allocation disagreement values of both methods have been measured and reported in Figure 4.Please note that this study focuses on the outcome of the quantity and allocation disagreement computation rather than the result of Kappa statistics due to the warnings (Pontius and Millones, 2011). It was found that the re-combined object based method gained more agreements than the pixel-based method. The quantity disagreement was improved from 2% to 1%, and the allocation disagreement was reduced from 3% to 2%. The three boxes in Figure 5 indicate the areas where the two indistinguishable classes were noticeably changed. For the purpose of visualization, magnified views of the three boxes are displayed below of Figure 5.

4. Discussion and Conclusion

The results in Table 3 and Figure 3 and the statistical tests confirm that the combination of the spectral and texture features can be used for improving the class separability between the two mangrove species (*Ra* and *Rm*). The overall accuracy improved from 92% to 97%. The producer accuracy of *Ra* significantly improved from 68% to 94% and the producer accuracy of RA improved from 94% to 95%. The quantity and allocation disagreement values (Figure 4) also confirmed this findings. The disagreement was reduced in both cases. It can thus be concluded that this study provides the first accurate method for differentiating between the two species using remote sensing technology (Vaiphasa et al., 2006, Koedsin and Vaiphasa, 2013). In the existing literature, a similar object-based method was used for mapping mangroves in other weather zones (Wang et al., 2004a).

The current study reports that reclassification in the specified undifferentiated areas can help resolve the mixed class problem. The correlation between this study and a past study (Wang et al., 2004a) suggests that the proposed method may be extended for refining mangrove mapping accuracy at the species level in complex mangrove communities in other areas. The edge-based segmentation method was chosen for this study because the edges of the small objects always connected and closed (Jin, 2012). However, there are other alternative segmentation methods such as the point-based and growing-region methods. The point-based technique is not suitable for remote sensing data because it does not consider the surrounding pixels (Schiewe, 2002). On the other hand, the growing-region is a standard method (Schiewe, 2002) that can substitute for the edge-based segmentation method. Unfortunately, the performance of different segmentation methods for mangrove species discrimination has never been tested in the existing studies (Wang et al., 2004a, Myingt et al., 2008 and Heumann, 2011a) and such a comparative test would be exhaustive and is beyond the scope of this study. Only multispectral bands were analyzed in this study because object-based classification cannot be processed on the difference spatial resolution without extra data transformation processing (i.e. fusing, resampling). The transformation of the image data could lead to errors the information and shape of the objects in segmentation (Schiewe, 2002). The panchromatic band, on the other hand, is undergoing investigation for canopy extraction methods (Zhang and Hu, 2012) to increase the species discrimination potential.

Furthermore, the use of ancillary data such as physiological parameters and vegetation indices are also underway. Detailed mangrove species mapping can provide useful information for mangrove forest management and recent trials on modern earth observation satellites have demonstrated the potential of remote sensing technology for mangrove species discrimination. Nevertheless, existing methods have been unable to differentiate between two dominant species, *Ra* and *Rm*. The method contained in this study effectively resolves this problem. The proposed object-based classification method provides accurate mangrove species discrimination of the two previously indistinguishable species and can be used for mangrove species classification in other Ra and Rm dominated areas. Additional data such as canopy shapes, physiological parameters, and vegetation indices may be integrated in the future studies to further improve the accuracy of results.

Acknowledgements

I would like to thank Faculty of Engineering, Chulalongkorn University for financial supports of this research (Faculty Research Funding).

Reference

Allouche, O., Tsoar, A. and Kadmon, R., 2006, Assessing the Accuracy of Species Distribution Models: Prevalence, Kappa and True Skill Statistic (TSS). *Journal of Applied Ecology*, 43,

1223–1232.

Almeida-Guerra, P., 2002, Use of SPOT Images as a Tool for Coastal Zone Management and Monitoring of Environmental Impacts in the Coastal Zone. *Optical Engineering*, 41(9), 2144-2151.

Alsaaideh, B., Al-Hanbali, A., Tateishi, R., Kobayashi, T. and Hoan, N. T., 2013, Mangrove Forests Mapping in the Southern Part of Japan using Landsat ETM+ with DEM. *Journal of Geographic Information System*, 5(4), 369-377.

Chadwick, J., 2011, Integrated LiDAR and IKONOS Multispectral Imagery for Mapping Mangrove Distribution and Physical Properties. *International Journal of Remote Sensing*, 32, 6765-6781.

Chauvaud, S., Bouchon, C. and Maniere, R., 2001, Thematic Mapping of Tropical Marine Communities (Coral Reefs, Seagrass Beds and Mangroves) using SPOT Data in Guadeloupe Island. *Oceanologica Acta*, 24, S3–S16.

Congalton, R. G. and Green, K., 2009, *Assessing the Accuracy of Remotely Sensed Data- Principles and Practices*, 2nd, (New York: CRC Press).

Foody, G. M., 2004, Thematic Map Comparison: Evaluating the Statistical Significance of Differences in Classification Accuracy. *Photogrammetric Engineering and Remote Sensing*, 70, 627–633.

Foody, G. M., 2008, Harshness in Image Classification Accuracy Assessment. *International Journal of Remote Sensing*, 29, 3137–3158.

Gao, J. A., 1999, Comparative Study on Spatial and Spectral Resolutions of Satellite Data in Mapping Mangrove Forests. *International Journal of Remote Sensing*, 20(14), 2823-2833.

Gao, J., Chen, H., Zhang, Y. and Zha, Y., 2004, Knowledge-Based Approaches to Accurate Mapping of Mangroves from Satellite Data. *Photogrammetric Engineering and Remote Sensing*, 11(70), 1241–1248.

Giri, C. and Muhlhausen, J., 2008, Mangrove Forest Distribution and Dynamics in Madagascar (1975–2005). *Sensors*, 8(4), 2104-2117.

Gray, C. D. and Kinnear, P. R., 2012, *IBM SPSS STATISTICS 19*, (United Kingdom: Psychology Press).

Green, E. P., Clark, C. D., Mumby, P. J., Edwards, A. J. and Ellis, A. C., 1998, Remote Sensing Techniques for Mangrove Mapping. *International Journal of Remote Sensing*, 19(5), 935–956.

Hardin, P. J. and Thomson, C. N., 1992, Fast Nearest Neighbor Classification Methods for Multispectral Imagery, *Professional Geographer*, 44(2), 191–202.

Heumann, B. W., 2011a, An Object-Based Classification of Mangroves using a Hybrid Decision Tree—Support Vector Machine Approach. *Remote Sensing*, 3(11), 2440-2460.

Heumann, B. W., 2011b, Satellite Remote Sensing of Mangrove Forests: Recent Advances and Future Opportunities. *Progress in Physical Geography*, 35(1), 87–108.

Hogarth, P. J., 1999, *The Biology of Mangroves*. (Oxford: Oxford University Press).

Huang, X., Zhang, L. and Wang, L., 2009, Evaluation of Morphological Texture Features for Mangrove Forest Mapping and Species Discrimination using Multispectral IKONOS Imagery. *IEEE Geoscience and Remote Sensing Letters*, 6(3), 393–397.

Jin, X., 2012, Segmentation-Based Image Processing System. U.S. Patent 8,260,048, filed Nov. 14, 2007, and issued Sept. 4, 2012.

Koedsin, W. and Vaiphasa, C., 2013, Discrimination of Tropical Mangroves at the Species Level with EO-1 Hyperion Data. *Remote Sensing*, 5, 3562-3582.

Kovacs, J. M., Wang, J. and Blanco-Correa, M., 2001, Mapping Disturbances in a Mangrove Forest using Multi-Date Landsat TM imagery. *Environment Management*, 27, 763-776.

Kuenzer, C., Bluemel, A., Gebhardt, S., Quoc, T. V. and Dech, S., 2011, Remote Sensing of Mangrove Ecosystems: A Review. *Remote Sensing*, 3, 878-928.

Li, Z., Hayward, R., Zhang, J., Jin, H. and Walker, R., 2010, Evaluation of Spectral and Texture Features for Object-Based Vegetation Species Classification using Support Vector Machines. In: Wagner W., Székely, B. (eds.): *ISPRS TC VII Symposium – 100 Years ISPRS*, Vienna, Austria, July 5–7, 2010, IAPRS, Vol. XXXVIII, Part 7A.

Manson, F. J., Loneragan, N. R., McLeod, I. M. and Kenyon, R. A., 2001, Assessing Techniques for Estimating the Extent of Mangroves: Topographic Maps; Aerial Photographs and Landsat TM Images. *Marine and Freshwater Research*, 52, 787–792.

Muttitanon, W. and Tripathi, N. K., 2005, Land use/land cover changes in Coastal Zone of Ban Don Bay, Thailand using Landsat 5 TM Data. *International Journal of Remote Sensing*, 26(11), 2311-2323.

Myint, S. W, Giri, C. P., Wang, L., Zhu Z. and Gillette S. C., 2008, Identifying Mangrove Species and Their Surrounding Land Use and Land Cover Classes Using an Object-Oriented Approach with a Lacunarity Spatial Measure. *GIScience and Remote Sensing*, 45(2), 188–208.

Neukermans, G., Guebas, F. D., Kairo, J. G. and Koedam, N., 2008, Mangrove Species and Stand Mapping in Gazi Bay (Kenya) using Quickbird Satellite Imagery. *Journal of Spatial Science*, 53(1), 75–86.

Pontius, Jr, R. G. and Millones, M., 2011, Death to Kappa: Birth of Quantity Disagreement and Allocation Disagreement for Accuracy Assessment. *International Journal of Remote Sensing,* 32(15): 4407-4429.

Saito, H., Bellan, M. F., Al-Habshi, A., Aizpuru, M. and Blasco, F., 2003, Mangrove Research and Coastal Ecosystem Studies with SPOT-4 HRVIR and TERRA ASTER in Arabian Gulf. *International Journal of Remote Sensing*, 24(21), 4073-4092.

Schiewe, J., 2002, Segmentation of High-Resolution Remotely Sensed Data-Concepts, Application and Problems. In: Armenakis, C., Lee, Y.C. (eds.): *ISPRS Commission IV, Symposium, Geospatial Theory, Processing and Applications*, Ottawa, Canada, July 9-12, 2002, IAPRS, Vol. XXXIV, Part 4.

Sirikulchayanon, P., Sun, W. and Oyana, T.J., 2008, Assessing the Impact of the 2004 Tsunami on magroves using Remote Sensing and GIS Techniques. *International Journal of Remote Sensing*, 29(12), 3553-3576.

Thu, P. M. and Populus, J., 2007, Status and changes of Mangrove Forest in Mekong Delta: Case Study in Tra Vinh, Vietnam. *Estuarine, Coastal and Shelf Science*, 71(1-2), 98-109.

Tomlinson, P. B. 1995. *The Botany of Mangroves*, (Cambridge: Cambridge University Press).

Tong, P. H., Auda, Y., Populus, J., Aizpura, M., Habshi, A. A. and Blasco, F., 2004, Assessment from Space of Mangroves Evolution in the Mekong Delta; in Relation to Extensive Shrimp Farming. *International Journal of Remote Sensing*, 25, 4795-4812.

Vaiphasa, C., Skidmore, A. K. and de Boer, W. F., 2006, A Post-Classifier for Mangrove Mapping using Ecological Data. *ISPRS Journal of Photogrammetry and Remote Sensing*, 4(75), 1–10.

Wang, L., Sousa, W. P. and Gong, P., 2004a, Integration of Object-Based and Pixel-Based Classification for Mapping Mangroves with IKONOS IMAGERY. *International Journal of Remote Sensing*, 25(24), 5655–5668.

Wang, L., Sousa, W. P., Gong, P. and Biging, G. S., 2004b, Comparison of IKONOS and Quickbird Images for Mapping Mangrove Species on the Caribbean Coast of Panama. *Remote Sensing of Environment*, 91(3-4), 432–440.

Wang, L., José, L., Cárdenas, S. and Sousa. W. P., 2008, Neural Network Classification of Mangrove Species from Multi-seasonal Ikonos Imagery. *Photogrammetric Engineering & Remote Sensing*, 74, 921–927.

Wang, L. and Sousa, W. P., 2009, Distinguishing Mangrove Species with Laboratory Measurements of Hyperspectral Leaf Reflectance. *International Journal of Remote Sensing*, 30(5), 1267–1281.

Zhang, K. and Hu, B., 2012, Individual Urban Tree Species Classification Using Very High Spatial Resolution Airborne Multi-Spectral Imagery Using Longitudinal Profiles. *Remote Sensing*, 4(6), 1741-1757.